# Ground Motions from the 2015 $M_w$ 7.8 Gorkha, Nepal, Earthquake Constrained by a Detailed Assessment of Macroseismic Data

by Stacey S. Martin, Susan E. Hough, and Charleen Hung

## ABSTRACT

To augment limited instrumental recordings of the $M_w$ 7.8 Gorkha, Nepal, earthquake on 25 April 2015 (Nepali calendar: 12 Baisakh 2072, Bikram Samvat), we collected 3831 detailed media and first-person accounts of macroseismic effects that include sufficiently detailed information to assign intensities. The resulting intensity map reveals the distribution of shaking within and outside of Nepal, with the key result that shaking intensities throughout the near-field region only exceeded intensity 8 on the 1998 European Macroseismic Scale (EMS-98) in rare instances. Within the Kathmandu Valley, intensities were generally 6–7 EMS. This surprising (and fortunate) result can be explained by the nature of the mainshock ground motions, which were dominated by energy at periods significantly longer than the resonant periods of vernacular structures throughout the Kathmandu Valley. Outside of the Kathmandu Valley, intensities were also generally lower than 8 EMS, but the earthquake took a heavy toll on a number of remote villages, where many especially vulnerable masonry houses collapsed catastrophically in 7–8 EMS shaking. We further reconsider intensities from the 1833 earthquake sequence and conclude that it occurred on the same fault segment as the Gorkha earthquake.

*Online Material:* Tables of locations with 1998 European Macroseismic Scale (EMS-98) intensity assignments for the 25 April 2015 Gorkha and the 26 August 1833 Nepal earthquakes.

## INTRODUCTION

The $M_w$ 7.8 Gorkha, Nepal, earthquake on 25 April 2015 took a heavy toll on Nepal, causing over 9000 deaths and leaving hundreds of thousands without shelter. Although similar and even larger megathrust earthquakes have occurred in the Himalayas as recently as 1950 (e.g., Chen and Molnar, 1977), the 2015 earthquake is the first to be captured by modern instrumentation. Key questions about ground motions also arose in the aftermath of the Gorkha earthquake, namely why damage in the Kathmandu Valley and other parts of Nepal was not more severe, despite the high magnitude of the event, the directivity of the rupture, its proximity to population centers, and the fragility of local, vernacular structures. Observations of this earthquake thus provide a unique and invaluable opportunity to quantify earthquake processes and seismic hazard associated with Himalayan earthquakes.

Although the earthquake was well recorded at regional and teleseismic distances, there is a paucity of critical instrumental data to constrain near-field ground motions. At the time of the mainshock, only a handful of strong-motion instruments were operating in Nepal (Dixit *et al.*, 2015). Data from four strong-motion instruments (Nobuo *et al.*, 2015) have not been made freely available. High data rate (5 Hz) Global Positioning Systems (GPS) data from a site in the Kathmandu Valley and an adjacent hard-rock site constrain coseismic particle displacements of up to 1.8 m amplitude with 5 mm precision and with a 0.4 Hz aliasing frequency but are insensitive to higher frequency, low-amplitude accelerations (Galetzka *et al.*, 2015). For the mainshock, the U.S. Geological Survey (USGS) ShakeMap relied largely on empirical ground-motion prediction equations to map out shaking intensities (Hayes *et al.*, 2015). The USGS Community Internet Intensity Map system (also known as "Did You Feel It?" [DYFI]; Wald *et al.*, 1999) has in recent years produced invaluable, spatially rich intensity data that are now used to augment instrumental data in ShakeMaps. Outside the United States and its territories, however, this system has limitations. DYFI data are sparse (Fig. 1a) for the Gorkha earthquake, and intensities were not assigned with a detailed consideration of building type. To constrain the intensity distribution more fully, in the weeks following the earthquake, we collected accounts from conventional news outlets and social media and interpreted intensities using the 1998 European Macroseismic Scale (EMS-98) in keeping with practices described by Martin and Szeliga (2010).

To assess the character and extent of the macroseismic field, and to maintain uniformity with previous studies (e.g., Martin and Szeliga, 2010), we utilized the EMS-98 scale (Grünthal, 1998). This supersedes the Medvedev–Sponheuer–Kárník (MSK) scale (Medvedev *et al.*, 1965) and is generally consistent with intensities that use the modified Mercalli intensity scale

 doi: 10.1785/0220150138

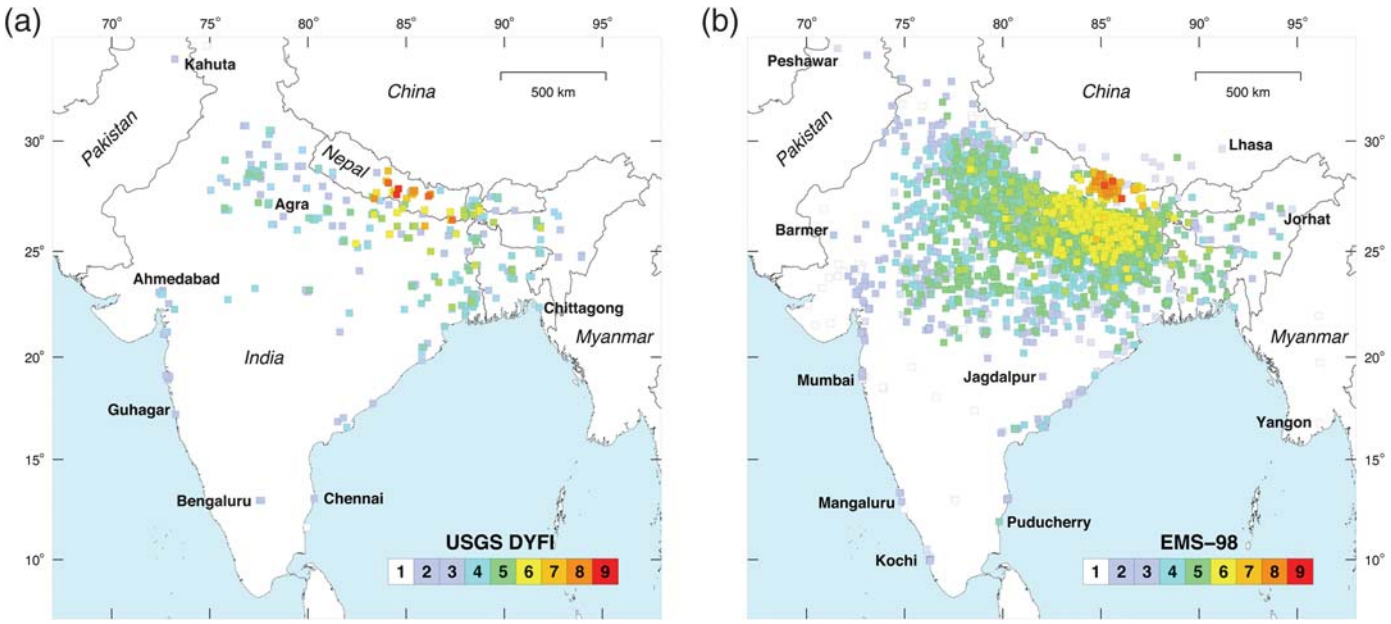


▲ **Figure 1.** (a) "Did You Feel It?" (DYFI) and (b) 1998 European Macroseismic Scale (EMS-98) intensities for the 25 April 2015 Gorkha earthquake.

(Musson *et al.*, 2010). We avoided assessing intensities at locations where ground deformation, liquefaction, or landslides were reported (Ambraseys and Douglas, 2004) and followed guidelines outlined by Martin and Szeliga (2010) for intensities in the 2–4 EMS range. Each intensity value was also assigned a quality weighting (Musson, 1998), in particular to identify location, and/or reliability uncertainties in the raw data. Within 21 large cities (population > 500, 000) in India and Nepal, such as Allahabad and Kathmandu, respectively, multiple press accounts were used, occasionally in conjunction with closed-circuit television (CCTV) footage, to assess and map intensity variations within the metropolitan area to distinguish site response (e.g., between fluvial and hard-rock sites). Within the range of intensities 3–5 EMS, media reports are often categorical when noting if people went or ran outdoors, sometimes in the absence of other qualifiers. In our experience with earthquakes in the Indian subcontinent (e.g., Martin and Kakar, 2012), we find there is a tendency for many people, including those who did not feel any shaking, to vacate buildings at lower intensities than might be stipulated in the EMS-98. In such cases, we assigned 3 EMS if people went outdoors, 4 EMS if people were frightened and went outdoors, and 4–5 EMS if they were frightened and ran outdoors.

Of particular note for our study, EMS includes extensive supporting materials and guidelines to distinguish between the severity (grades) of damage to different construction types by using vulnerability classes (Grünthal, 1998). This aspect of the scale is critical for reliable assessment of intensities from the Gorkha earthquake because apparently catastrophic damage (i.e., complete collapse equivalent to grade 5 damage) of vulnerable masonry buildings tend to saturate above MSK VII–VIII (Ambraseys and Douglas, 2004), equivalent to 7–8 EMS. Shaking severity of 8 EMS, for example, corresponds to widespread moderate damage (grade 2) to reinforced cement concrete (RCC; type C) buildings without earthquake resistant designs. At 9 EMS, people may be forcibly thrown to the ground, and many RCC buildings experience heavy (grade 3) damage.

We collected reports of the earthquake from 3831 locations, 3411 of which had both reliable geographic coordinates and contained sufficient information to assess intensities (Fig. 1b; Ⓔ Table S1, available in the electronic supplement to this article), as outlined above. The mainshock was felt throughout Nepal, in southern Tibet, and in many parts of the Indian subcontinent. As noted by Martin and Hough (2015), Figure 1b underscores the need to undertake traditional surveys to supplement data from regions poorly sampled by modern online questionnaires such as the DYFI, either through lack of awareness or poor Internet access. In contrast to the DYFI map, our results found the earthquake was more widely felt in peninsular India.

The greatest damage (≥ 7 EMS) occurred within Nepal and extended approximately 250 km eastward along the Himalayan arc. Shaking approached or equaled 8 EMS at only a few places, including Archale (28.017° N, 85.177° E), where eyewitnesses were repeatedly thrown to the ground (Ⓔ Table S1). Traverses along roads and visits by helicopter to remote regions near the epicenter indicated that 6–7 EMS prevailed above most of the rupture zone with pockets of 8 EMS locally confined to ridges (Roger Bilham, personal comm., 2015). In the Nepali Terai along the border with India, the shock elicited panic and resulted in modest damage (6 EMS). In mountains to the west of the epicenter in Nepal, shaking decayed rapidly. It is important to note, however, that intensities were systematically higher in adjacent parts of the plains of northern India. This amplification is qualitatively consistent with observed

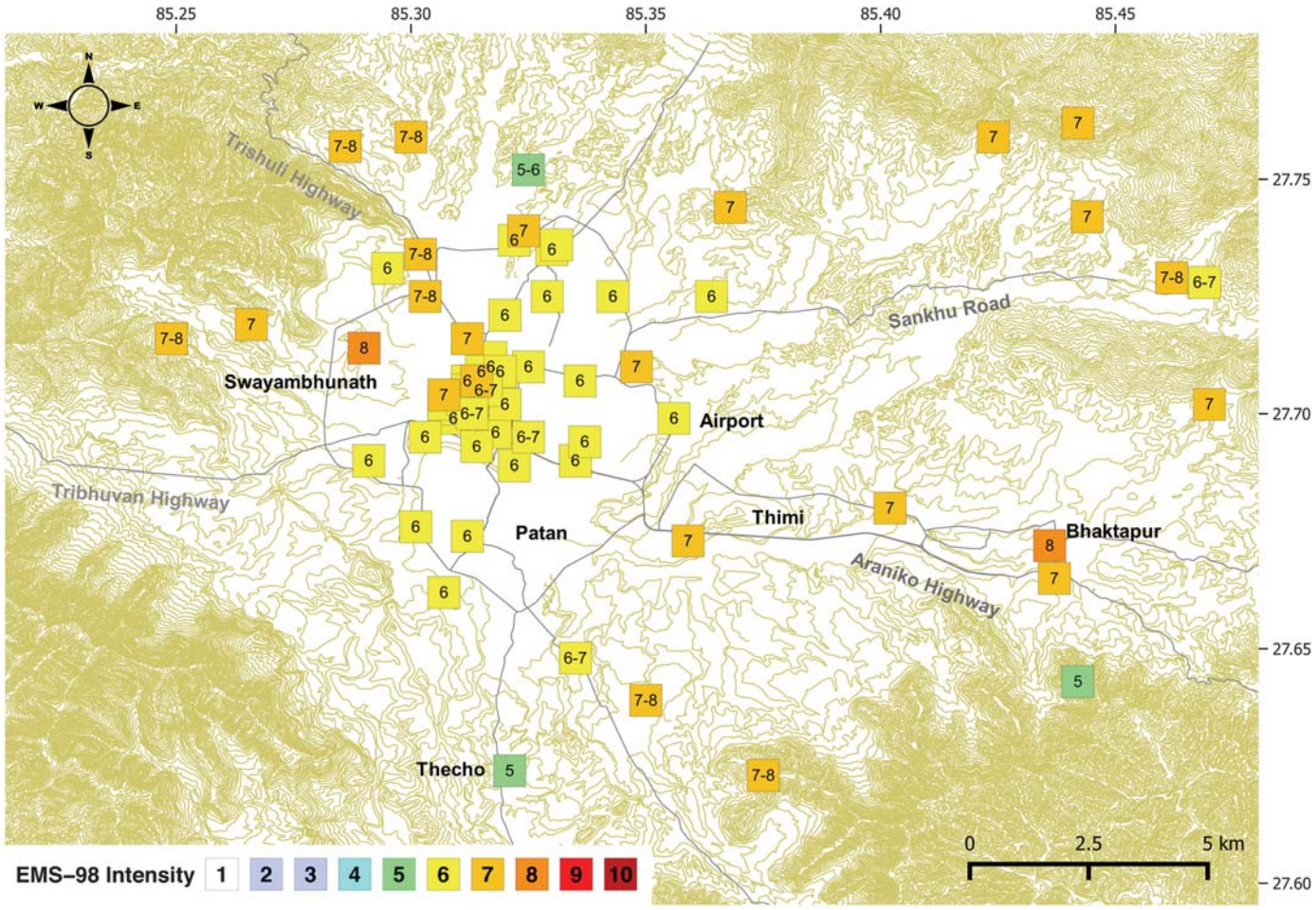


▲ **Figure 2.** EMS-98 intensities for the Gorkha earthquake in the Kathmandu Valley. Main roads are shown, as are topographic contours.

amplification of macroseismic intensities in geosynclinal sediments of the Gangetic foredeep during the 15 January 1934 $M_w \approx 8.4$ Nepal–Bihar earthquake (Dunn *et al.*, 1939; Hough and Bilham, 2008).

Few intensity observations above the rupture zone northeast of Kathmandu were made prior to the $M_w$ 7.3 Dolakha earthquake on 12 May 2015, and those we have included were obtained from media accounts and from photographic evidence published prior to this aftershock. Preliminary intensity data for the mainshock are currently available from Tibet in the region 50 km north of the aftershock (Anonymous, 2015), but our assessments of damage in similar locations based on photographic documentation yield lower EMS intensity values than suggested by these authors. Similarly, in the Langtang Valley where eyewitnesses had no difficulty standing on the valley floor during the mainshock, personal accounts supplemented by video and still photographs establish that damage (6–7 EMS) occurred in the village of Kyanjin Gompa (28.214° N, 85.524° E) as a result of the mainshock, prior to the destruction of buildings 30 s later by the wind blast from the debris avalanche that destroyed the village of Langtang (Roger Bilham, personal comm., 2015). In contrast, accounts from mountaineers 1000 m above the valley floor at Tserko Ri (28.213° N, 85.600° E) report being thrown down by the shaking, suggesting that 8 EMS may have prevailed at higher elevations.

Damage in the Kathmandu Valley, corresponding to 6–7 EMS (Fig. 2), was lower than expected given the proximity of the valley to the rupture (Hayes *et al.*, 2015). In the first 10 s of strong ground motion in the Kathmandu Valley, displacements exceeded 1.5 m and velocities instantaneously exceeded 50 cm/s (Dixit *et al.*, 2015; Galetzka *et al.*, 2015), which resulted in many people being unable to stand, a feature of 8 EMS, despite surrounding building damage characteristic of 6–7 EMS. Small pockets of locally higher damage occurred at sites on ridges or hills, including at the Swayambhunath Temple, and in areas near where liquefaction was reported. At the Swayambhunath Temple (Fig. 3a), unreinforced brick buildings (vulnerability class B) surrounding the central stupa (central shrine) experienced significant structural damage (grade ≥ 4), indicating 8 EMS. In stark contrast, in the Thecho area (Fig. 3b) in the southern valley, a very well-built RCC house was undamaged and precariously placed knick-knacks were not displaced with the exception of a single plaster mask. This mask had been balanced precariously on a shallow windowsill from which it fell and broke, indicating the level of shaking here approached but did not exceed 5 EMS.


▲ **Figure 3.** (a) Damage (grade 4–5) to substantial brick building within the Swayambhunath temple complex; (b) undamaged house in the Thecho area, where all precariously placed objects, with one exception, were unaffected.

In India, the earthquake was felt extensively between 75° E and 95° E, but intensities rapidly diminished south of ~22° N. Significant damage (including the collapse of poorly built masonry or mud (kaccha) walls, the fall of masonry parapets or balcony railings, and damage to tall, free-standing structures such as minarets, steeples, mobile telecommunication towers, and chimneys at brick kilns) was reported from within ~500 km of the epicenter. Noteworthy areas of anomalously high intensities were observed within this zone, for example, in the vicinity of Agra. Although the mausoleum itself was undamaged, small pieces of stone work fell from a building in the forecourt of the Taj Mahal (Amar Ujala, 26 April 2015). The Taj Mahal is said to have sustained injury in an earthquake in the late 18th century (Parkes, 1850) but was unaffected by the 1905 Kangra (Middlemiss, 1910) and 1934 Nepal-Bihar earthquakes (Dunn *et al.*, 1939). Outside this region, shaking was mainly felt in multistoried buildings along the western and eastern coasts of India at distances in excess of 1300 km, with the farthest report being from Kochi in the state of Kerala, at a distance of 2200 km. To the west, it was perceived as far as Peshawar and in the east at Jorhat (Fig. 1b). It was also reportedly felt on offshore drilling platforms near Kakinada (16.987° N, 82.247° E) on the east coast of India and underground by some in a mine at Tetulmari (23.814° N, 86.343° E) on the Chota Nagpur plateau. The outer extremities of the felt area are well constrained, with the exception to the southeast in Myanmar, although reliable accounts noted that shaking was not felt in Mandalay, Naypyidaw, or Yangon.

Seismic seiches, some fatal, were noticed at many places in Bangladesh and were also observed in rivers, lakes, and reservoirs in central, eastern, and northeastern India, the farthest report in the west being from Sheopur (25.670° E, 76.669° E) in the Chambal Valley and to the east at Borkola (26.931° N, 94.740° E) in upper Assam. The earthquake also produce a noticeable hydrogeologic response at Bela (26.788° N, 85.728° E) and Parihar (26.722° N, 85.676° E) in India, where hand pumps became artesian following the earthquake (Dainik Jagran, 26 April 2015). Amateur video filmed after the mainshock in Hansaposa–Tarahara (26.693° N, 87.256° E) in the Sunsari district, Nepal, recorded the same phenomenon alongside liquefaction (https://www.youtube.com/watch?v=rVZ0V_PjuNo; last accessed June 2015). Aquifers were also disturbed at far-field locations, as evidenced by reports of borewells and natural springs turning muddy or milky in Jagdalpur (19.069° N, 82.030° E), Mirzapur (25.170° N, 82.564° E), Peterbar (23.615° N, 85.851° E), Rajgir (25.170° N, 85.416° E), and Rewa (24.530° N, 81.300° E).

Reports of liquefaction were available from southern Nepal and from isolated locations in all of the border districts in the Indian state of Bihar between 84° E and 88° E.

## RESULTS

We first consider the decay of observed intensities with distance. Although nearest-fault distance would be more physically meaningful, for the initial analysis presented here we rely on epicentral distance so that the results can be compared to an existing intensity-prediction equation based on epicentral distance. From the intensity database compiled by Martin and Szeliga (2010), Szeliga *et al.* (2010) developed separate intensity-prediction equations for the Himalayan region and for peninsular India. In Figure 4, we show the media-based intensities for the Gorkha earthquake, together with predicted intensities using the Szeliga *et al.* (2010) Himalayan model for an intensity magnitude ($M_I$) of 7.8. Figure 4 also shows EMS-98 intensities for the $M_w \approx 8.4$ Nepal–Bihar earthquake in 1934 (Martin and Szeliga, 2010).

Observed intensities are generally consistent with values predicted by the Szeliga *et al.* (2010) Himalayan model given $M_I$ 7.8, but they are systematically lower at near-field distances. As noted, following Szeliga *et al.* (2010), we consider only epicentral distances. Estimated intensities for near-field locations including Kathmandu would clearly be even more anomalously low if one considered nearest-fault distance (< 12 km beneath

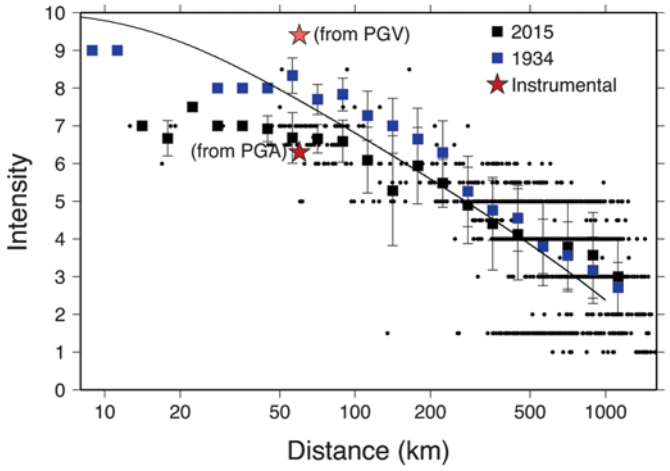


▲ **Figure 4.** Media-based intensities as a function of epicentral distance (black dots), and bin-averaged values (black squares) with one-sigma uncertainties. Also shown are intensities for the 1934 Nepal–Bihar earthquake, from Martin and Szeliga (2010), and estimated intensities for the Kathmandu Valley from instrumental data using both the peak ground velocity–based (light red star) and peak ground acceleration–based (dark red star) relations of Wald *et al.* (1999). Line indicates predicted intensities using Himalaya model of Szeliga *et al.* (2010) for $M_l$ 7.8.

the city). Instrumental intensities (Fig. 4) can be determined from a strong-motion recording in Kathmandu (Dixit *et al.*, 2015) using the Wald *et al.* (1999) relationships between intensity and both peak ground velocity (PGV) and peak ground acceleration (PGA). These relations yield quite different intensity values, intensity 6.3 (PGA) versus 9.4 (PGV). Although Wald *et al.* (1999) concluded that the PGV relationship is more appropriate for strong shaking (intensities above 7), that is not the case here. That is, the PGV–intensity relationship from Wald *et al.* (1999), while more consistent with expectations, is not consistent with observed damage and intensities from the Gorkha earthquake. The low macroseismic intensities in the Kathmandu Valley were due to the long-period character of the mainshock ground motions, which were strongly peaked at periods of approximately 5 s, without a strong basin response at shorter periods (Avouac *et al.*, 2015; Dixit *et al.*, 2015). Buildings in the Kathmandu Valley are commonly less than 5 stories tall, with expected natural periods no longer than 0.5 s. During the past decade a small number of taller buildings have been constructed, with heights of 10–17 stories. There is a widespread observation by the local population that the largest buildings, including the new high-end, 17-story Park View apartment complex (27.739° N, 85.324° E), sustained more severe damage than did the ubiquitous smaller buildings.

Near-field shaking intensities from the Gorkha earthquake were lower than predicted from well-calibrated intensity prediction equations. There is no possibility that the difference reflects any inconsistency in intensity values, because accounts of both the Gorkha earthquake and the calibration events were consistently interpreted by the first author. Moreover, the Himalayan model of Szeliga *et al.* (2010) was developed specifically for the region. As discussed by Hough (2013) and Martin and Hough (2015), who examined the $M_w$ 5.9 Bay of Bengal earthquake in 2014, differences between observed intensities and model predictions must thus reflect properties of the source itself. In a simplistic sense, systematically low intensities are commonly taken as an indication of a low-stress-drop source. In this case, it remains an open question why the mainshock ground motions were relatively depleted in 0.5–2 Hz energy. In any case, available strong-motion data, high-rate GPS data (Galetzka *et al.*, 2015), and CCTV videos of mainshock shaking reveal that near-field radiated energy from the Gorkha earthquake was dominated by long-period energy at ≈5 s. For example, in many cases, people, vehicles, or contents of structures were seen to be rocked by a strong, coherent pulse with an approximately 5 s period. This predominant long-period energy can be explained as a combination of source effects and nonlinear response of the Kathmandu Valley (Dixit *et al.*, 2015).

## IMPLICATIONS FOR HISTORICAL EARTHQUAKES

Our results have implications for the analysis of historical earthquakes, which we discuss briefly here. In Figure 5, we compare our intensities for the Gorkha earthquake with intensities from Martin and Szeliga (2010) for the 1934 Nepal–Bihar earthquake (Nepali calendar: 2 Magh 1990 Bikram Samvat). The magnitude of the 1934 earthquake was revised upward from $M_w$ 7.9 (Chen and Molnar, 1977) to $M_w \approx 8.4$ (Molnar and Qidong, 1984). Rupture parameters for the 1934 earthquake, including the precise magnitude, remain uncertain, and the epicenter was relocated (Chen and Molnar, 1977) using early instrumental data. On the basis of palaeoseismic observations and geomorphic markers of uplift a minimum rupture length of ~150 km is inferred between 85.85° E and 87.31° E but this does not exclude the possibility that the rupture might have extended farther to the east and west, amounting to a total rupture length of ~200–250 km (Sapkota *et al.*, 2013; Bollinger *et al.*, 2014). The rupture length is consistent with along-strike dimensions inferred from leveling data in Bihar (Bilham *et al.*, 1998). The full rupture area and slip distribution, however, are not constrained by geodetic data across the rupture. Rupture parameters from the Gorkha earthquake are constrained by finite-fault modeling (Hayes *et al.*, 2015). It is clear from Figure 5 that, relative to the Gorkha earthquake, damaging shaking from the 1934 earthquake extended farther south into Nepal and northern India. This difference can be explained readily as a consequence of the difference between the two events, namely that the 1934 event was a larger earthquake that ruptured the entire décollement and its frontal thrust (Sapkota *et al.*, 2013; Bollinger *et al.*, 2014), whereas the $M_w$ 7.8 Gorkha earthquake was restricted to the deeper 60% of the décollement with no coseismic rupture of the Main Frontal fault (Avouac *et al.*, 2015).

As discussed by Martin and Hough (2015), in the absence of instrumental data, intensity data for historical earthquakes

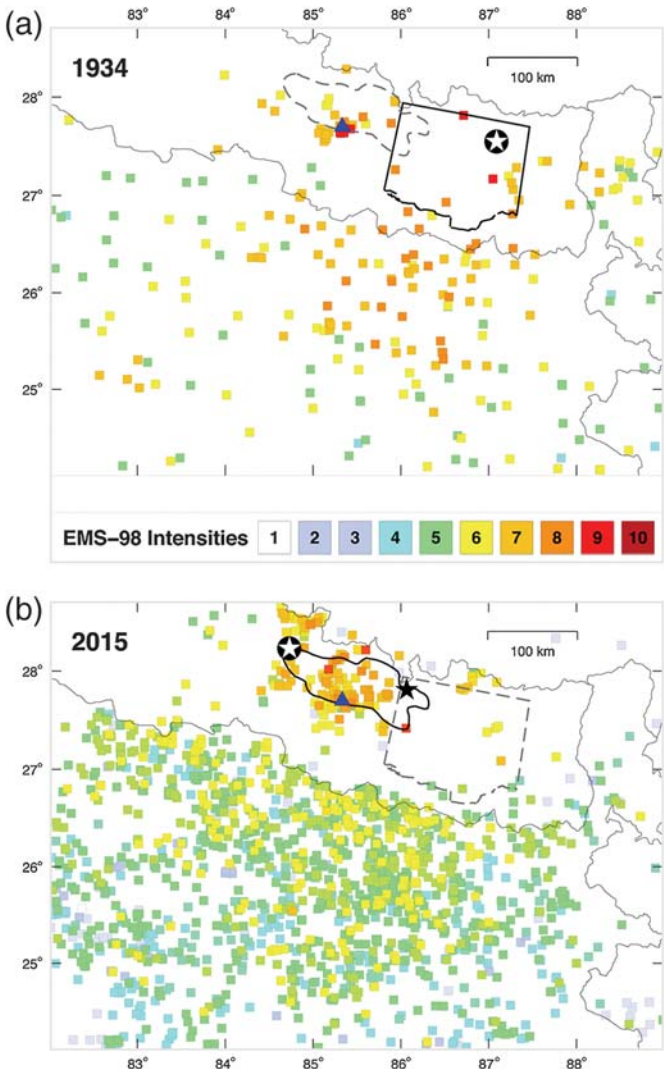


▲ **Figure 5.** (a) Intensity distribution (squares; colored scale as shown) for the 1934 Nepal–Bihar earthquake (Martin and Szeliga, 2010). The approximate rupture area of the 1934 earthquake is represented by a solid black line (Sapkota *et al.*, 2013; Bollinger *et al.*, 2014), and the rupture area of the 2015 earthquake is outlined with a dashed gray line (Lindsey *et al.*, 2015). The white star represents the location of the mainshock from Chen and Molnar (1977). (b) Intensity distribution for the Gorkha earthquake. The white star represents the Gorkha mainshock on 25 April 2015, and the black star represents the 12 May aftershock. The blue triangle is the location of Kathmandu.

can be used to calculate an intensity magnitude ($M_I$) that can differ from $M_w$ depending on the detailed source properties of an event. Martin and Hough (2015) demonstrate that the analysis of intensity data can significantly underestimate $M_w$ for some historical Himalayan earthquakes. Making the reasonable assumptions that some past large Himalayan earthquakes had similar rupture mechanisms and radiated energy as the Gorkha event, the magnitudes of such events in the historical record would likely be underestimated. In particular, large Himalayan earthquakes with estimated magnitudes ($M_w$) larger than 7.5 (Bilham and Ambraseys, 2005), such as those in Kashmir ($M_w \sim 7.6$, 1555), Kumaon ($M_w \sim 8.1$, 1803), central Nepal ($M_w \sim 7.7$, 1833), and Kangra ($M_w \sim 7.8$, 1905), generated no known surface rupture and thus may represent earthquakes with rupture processes similar to the Gorkha event. Additionally, in central Nepal, historical earthquakes with no reported surface rupture are reported to have caused damage in Kathmandu in 1408, 1681, 1767, 1808, 1826, and 1866, but there is insufficient information about any of these events to estimate their rupture zones (Anonymous, 1827; Rana, 1934; Chitrakar and Pandey, 1986; Pant, 2002).

It is especially interesting to reconsider the 26 August 1833 (Nepali calendar: 12 Bhadra 1890, Bikram Samvat) earthquake sequence in light of our results. Its magnitude has been estimated previously between $7.3 < M_I < 7.7$ (Bilham, 1995; Ambraseys and Douglas, 2004; Szeliga *et al.*, 2010). Its intensity distribution (Ⓔ Tables S2–S4) and the locations of inferred macroseismic epicenters (Bilham, 1995; Min, 1995; Ambraseys and Douglas, 2004; Szeliga *et al.*, 2010) were to the east of the 2015 epicenter (Fig. 6a). Although damage in southern Tibet in both events was severe, the impact of the two earthquakes was quite different in the Gorkha District. In 2015, heavy damage was sustained by Gorkha and in the surrounding villages (Roger Bilham, personal comm., 2015), whereas in 1833 only two houses collapsed in Gorkha (Campbell, 1833). Moreover, the region to the east of the Trishuli Gandaki river (~85° E) was reportedly significantly affected in 1833 (Rana, 1934). Although observed damage from the 2015 event is explained primarily by fragility of local masonry construction, with intensities generally no higher than 8 EMS, similar vulnerable construction materials and methods would have been prevalent in 1833, signifying that shaking in 1833 west of Kathmandu cannot have been as strong as during the recent event. The rupture zones and slip parameters of the two earthquakes therefore cannot be identical. Slip in the 2015 earthquake, however, is consistent with the release of 3.2 m of accumulated slip at the present-day convergence rate of 17.8 ± 0.5 mm/yr (Ader *et al.*, 2012) and the elapsed 182 years. The mainshock in 1833 at 23:56 local time was preceded by two strong earthquakes with increasing severity, first at sundown and then at ~23 : 35 local time (Campbell, 1833; Bilham, 1995), that brought people from their homes, a factor that was responsible for the low loss of life in Nepal, despite an estimated 18,000 buildings being destroyed in the entire kingdom (Rana, 1934) and over 4000 buildings collapsing in or near the Kathmandu Valley (Campbell, 1833; Rana, 1934), including 70% of the structures in Bhaktapur (Campbell, 1833). The 1833 earthquake was followed by three months of notable aftershocks (Bilham, 1995), including significant events on 4 October 1833, 18 October 1833, and 26 November 1833, which were strongly felt in the Kathmandu Valley (Campbell, 1833; Rana, 1934). The two aftershocks in October 1833 were also widely perceptible in the Gangetic plains as far as Chittagong and Jabalpur (Campbell, 1833; Bilham, 1995). The Nepali date (1891 Bikram Samvat) for 1834 is incorrectly recorded as 1835 in the

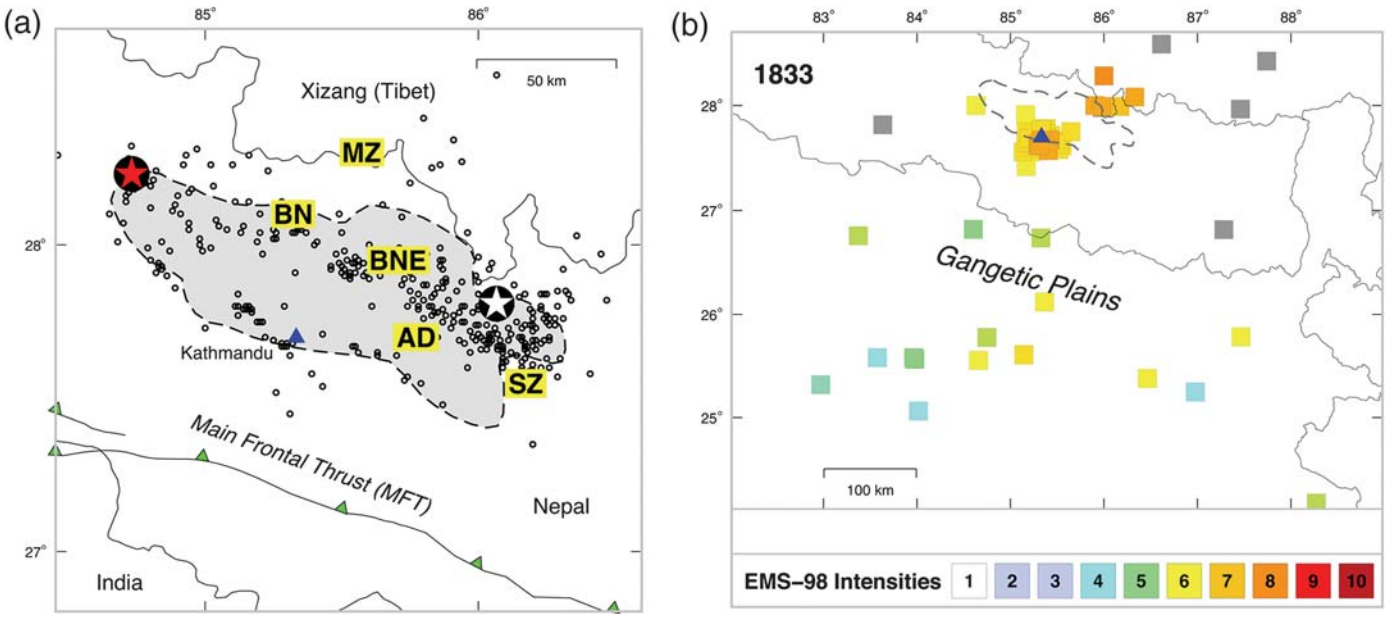


▲ **Figure 6.** (a) Mainshock (red star), 12 May aftershock (white star), and aftershocks of the 2015 earthquake (black circles 7.8 > $M_w$ > 4.0, 25 April–13 June) from the Nepal Seismic Network. Gray shading approximates the 2015 rupture zone. The blue triangle denotes the Kathmandu Valley. The sources of the estimated epicentral locations for the 1833 earthquake are indicated: MZ, Min (1995); BN and BNE, Bilham (1995); AD, Ambraseys and Douglas (2004); and SZ, Szeliga *et al.* (2010). (b) Spatial distribution of intensities (colored boxes) from the 1833 mainshock.

English translation of Rana (1934), thus misplacing the three aftershocks on 20 June 1834, 26 July 1834, and in late September 1834 that were also felt in the Kathmandu Valley. Of these, the earthquake in June caused seven fatalities in the Rongxar region, damaged the Dophenling monastery, and was followed by locally felt aftershocks in southern Tibet (Chen, 1982). Efforts (in 2011 by the first author) to locate additional official correspondence from the British political resident in Kathmandu for 1833 and 1834 (Nepal Residency Records, IOR/R/5/95-96) were futile.

Although the 1833 and 2015 events must have differed in detail, the apparent similarity of their magnitudes and their approximate correspondence in areas of high intensity suggests that the 1833 earthquake may have on the same segment of the décollement. Further work will be needed to reassess the magnitude of the 1833 earthquake in light of the observations from this study. It is possible that earlier moderately large historical earthquakes including some of the aforementioned historical earthquakes represent similar ruptures of this segment. We note, however, that such earthquakes do not involve slip of the interface to the south of 2015 rupture zone, suggesting that infrequent larger earthquakes must occur.

## CONCLUSIONS

We present spatially rich intensity data for the $M_w$ 7.8 Gorkha earthquake, determined from an exhaustive search of media accounts from the Indian subcontinent following the earthquake and supplemented by numerous first-hand observations close to the rupture zone. EMS-98 intensities were assigned for each account using modern conservative practices (e.g., Ambraseys and Douglas, 2004); of particular note, these assignments are consistent with those of Martin and Szeliga (2010), who undertook a comprehensive reinterpretation of the Indian historical catalog. In this study, we show that near-field intensities for the 2015 earthquake are significantly lower than predicted using the $M_I$ evaluation equations developed by Szeliga *et al.* (2010). The character of the Gorkha mainshock rupture, which gave rise to ground motions with a predominant period of ≈5 s (Dixit *et al.*, 2015; Galetzka *et al.*, 2015), provides an explanation for the low intensities. Intensities at distances of roughly 50–200 km were lower than those generated by the 1934 $M_w \approx 8.4$ Nepal–Bihar earthquake, which ruptured the adjacent segment of the plate boundary to the east. We infer that an earthquake in 1833, previously assigned $7.3 < M_I < 7.7$ (Bilham, 1995; Ambraseys and Douglas, 2004; Szeliga *et al.*, 2010), likely ruptured a similar segment of the décollement beneath the Himalayas. The 2015 earthquake may thus represent partial or complete rupture of this segment of the Himalayas, releasing cumulative convergence at currently observed geodetic rates. The spatially rich data for the Gorkha earthquake provide a valuable complement to the sparse set of instrumentally recorded accelerations for the Gorkha earthquake and promise to provide an important calibration event with which to re-evaluate previous Himalayan earthquakes for which only intensity data are available.

## DATA AND RESOURCES

Ⓔ Intensity data, also available in ASCII format, were assessed from primary sources listed in the Sources column of Tables S1–

S4. Summary responses from the U.S. Geological Survey "Did You Feel It?" questionnaire are free to download in various formats at http://earthquake.usgs.gov/earthquakes/eventpage/us20002926 (last accessed June 2015). Closed-circuit television and amateur videos utilized by this study are available at https://www.youtube.com/channel/UCoUAp8sJlurhws_dCCPAcDw (last accessed June 2015). The Nepal Survey Department topographic contour data used in Figure 2 are freely available at https://data.hdx.rwlabs.org/dataset/nepal-contour-lines-cod (last accessed June 2015). Figures were generated using Generic Mapping Tools (Wessel and Smith, 1991) and QGIS 2.8.2 (http://www.qgis.org, last accessed June 2015).

## ACKNOWLEDGMENTS

We thank those who provided felt-report questionnaires, as well as Sujan Raj Adhikari, Deepak Bhandari, Mukunda Bhattarai, Roger Bilham, Laurent Bollinger, Roser-Hoste Colomer, Sanjana Dalmiya, Royden D'Souza, Ankit Joshi, Priyanka Joshi, John Galetzka, Vineet Gahalaut, Ratnamani Gupta, Dannie Hidayat, Sorvigenaleon Ildefonso, Ellen Knappe, Phyo Maung Maung, Jaiganesh Murugesan, Suman Pariyar, Yvonne Soon, and Nang Thin Zar Win for eyewitness and photographic accounts of damage from the region. Kapil Timilsina and Shamik Mishra at the Madan Puraskar Pustakalaya (Patan) helped us to obtain a copy of the original Nepali version of Rana (1934). Deepa Mele Veedu and Manoj Deshpande translated Telegu news reports, and Çağıl Karakaş provided digitized traces of the 1934 rupture from Sapkota *et al.* (2013) and of the Main Frontal thrust. We also thank Alison Bird, Judith Hubbard, Çağıl Karakaş, Julian Lozos, Eric Thompson, and two anonymous reviewers for constructive comments that improved this manuscript.

S. S. M. was supported by the National Research Foundation (NRF) Singapore under its Singapore NRF Fellowship scheme (NRF Number NRF-NRFF2013-06) and by the Earth Observatory of Singapore, NRF Singapore, and the Singapore Ministry of Education under the Research Centres of Excellence initiative. S. E. H. was supported by the Office of U.S. Foreign Disaster Assistance, a branch of the U.S. Agency for International Development. This is EOS paper number 101.

## REFERENCES

Ader, T., J.-P. Avouac, J. Liu-Zeng, H. Lyon-Caen, L. Bollinger, J. Galetzka, J. Genrich, M. Thomas, K. Chanard, S. N. Sapkota, S. Rajaure, P. Shreshtha, L. Ding, and M. Flouzat (2012). Convergence rate across the Nepal Himalaya and interseismic coupling on the Main Himalayan thrust: Implications for seismic hazard, *J. Geophys. Res.* **117,** no. B04403, doi: 10.1029/2011JB009071.

Ambraseys, N., and J. J. Douglas (2004). Magnitude calibration of north Indian earthquakes, *Geophys. J. Int.* **159,** no. 1, 165–206, doi: 10.1111/j.1365-246X.2004.02323.x.

Anonymous (1827). *Asiatic Journal and Monthly Register for British India and Its Dependencies*, Vol. 23, January–June 1827, London, United Kingdom, 672–673.

Anonymous (2015). Tibet earthquake information, Nepal earthquake: China Earthquake Administration release of Nepal M=8.1 seismic intensity map, http://www.eq-xz.net/newweb/showart.asp?id=1907 (last accessed July 2015) (in Chinese).

Avouac, J.-P., L. Meng, S. Wei, T. Wang, and J.-P. Ampuero (2015). Lower edge of locked Main Himalayan Thrust unzipped by the 2015 Gorkha earthquake, *Nature* **8,** 708–711, doi: 10.1038/ngeo2518.

Bilham, R. (1995). Location and magnitude of the 1833 Nepal earthquake and its relation to the rupture zones of contiguous great Himalayan earthquakes, *Curr. Sci.* **69,** no. 2, 155–187.

Bilham, R., and N. N. Ambraseys (2005). Apparent Himalayan slip deficit from the summation of seismic moments for Himalayan earthquakes, 1500–2000, *Curr. Sci.* **88,** no. 10, 1658–1663.

Bilham, R., F. Blume, R. Bendick, and V. K. Gaur (1998). Geodetic constraints on the translation and deformation of India: Implications for future great Himalayan earthquakes, *Curr. Sci.* **74,** no. 3, 213–229.

Bollinger, L., S. N. Sapkota, P. Tapponnier, Y. Klinger, M. Rizza, J. Van der Woerd, D. R. Tiwari, R. Pandey, A. Bitri, and S. Bes de Berc (2014). Estimating the return times of great Himalayan earthquakes in eastern Nepal: Evidence from the Patu and Bardibas strands of the Main Frontal Thrust, *J. Geophys. Res. Solid Earth* **119,** 7123–7163, doi: 10.1002/2014JB010970.

Campbell, A. (1833). Further particulars of the earthquake in Nepal, *J. Asiatic Soc. Bengal* **2,** Misc. VI, 636–639.

Chen, J. (Editor) (1982). *A Collection of Material on Earthquakes in Tibet: 642–1980*, Vol. 1, Science and Technology Committee of Tibet Autonomous Region, Tibet People's Publishing House, Lhasa, Tibet Autonomous Region of the People's Republic of China, 39–76 (in Chinese).

Chen, Y.-P., and P. Molnar (1977). Seismic moments of major earthquakes and the average rate of slip in central Asia, *J. Geophys. Res.* **82,** 2945–2969, doi: 10.1029/JB082i020p02945.

Chitrakar, G. R., and M. R. Pandey (1986). Historical earthquakes of Nepal, *Bull. Nepal Geol. Soc.* **4,** 7–8.

Dixit, A. M., A. Ringler, D. Sumy, E. Cochran, S. E. Hough, S. S. Martin, S. Gibbons, J. Luetgert, J. Galetzka, S. N. Shrestha, *et al.* (2015). Strong motion observations of the **M** 7.8 Gorkha, Nepal, earthquake sequence and development of the N-SHAKE strong-motion network, *Seismol. Res. Lett.* **86,** no. 6, doi: 10.1785/0220150146.

Dunn, J. A., J. B. Auden, A. M. N. Ghosh, S. C. Roy, and D. N. Wadia (1939). The Bihar–Nepal earthquake of 1934, *Memoirs of the Geological Survey of India*, **37,** 891.

Galetzka, J., D. Melgar, J. F. Genrich, J. Geng, S. Owen, E. O. Lindsey, X. Xu, Y. Bock, J.-P. Avouac, L-B. Adhikari, *et al.* (2015). Slip pulse and resonance of Kathmandu basin during the 2015 $M_w$ 7.8 Gorkha earthquake, Nepal, imaged with space geodesy, *Science* **349,** no. 6252, 1091–1095, doi: 10.1126/science.aac6383.

Grünthal, G. (Editor) (1998). The European Macroseismic Scale EMS-98, Vol. 15, Conseil de l'Europe, Cahiers du Centre Europeén de Geodynamique et de Seismoligie, Luxembourg, 101 pp.

Hayes, G. P., W. Barnhart, R. Briggs, W. Yeck, D. E. McNamara, D. Wald, J. Nealy, H. Benz, R. Gold, K. Jaiswal, *et al.* (2015). Rapid characterization of the 2015 $M_w$ 7.8 Nepal (Gorkha) earthquake, *Seismol. Res. Lett.* **86,** no. 6, doi: 10.1785/0220150145.

Hough, S. E. (2013). Spatial variability of "Did You Feel It?" intensity data: Insights into sampling biases in historical earthquake intensity distributions, *Bull. Seismol. Soc. Am.* **93,** doi: 10.1785/0120120285.

Hough, S. E., and R. Bilham (2008). Site response of the Ganges basin inferred from re-evaluated macroseismic observations from the 1897 Shillong, 1905 Kangra, and 1934 Nepal earthquakes, *J. Earth Syst. Sci.* **117,** 773–782, doi: 10.1007/s12040-008-0068-0.

Lindsey, E. O., R. Natsuaki, X. Xu, M. Shimada, M. Hashimoto, D. Melgar, and D. T. Sandwell (2015). Line-of-sight displacement from ALOS-2 interferometry: $M_w$ 7.8 Gorkha earthquake and $M_w$ 7.3 aftershock, *Geophys. Res. Lett.* **42,** 6655–6661, doi: 10.1002/2015GL065385.

Martin, S., and S. E. Hough (2015). The 2014 Bay of Bengal earthquake: Macroseismic data reveals a high-stress drop event, *Seismol. Res. Lett.* **86,** no. 2A, 369–377, doi: 10.1785/0220140155.

Martin, S., and D. M. Kakar (2012). The 19 January 2011 $M_w$ 7.2 Dalbandin earthquake, Balochistan, *Bull. Seismol. Soc. Am.* **100,** no. 4, 1810–1819, doi: 10.1785/0120110221.

Martin, S., and W. Szeliga (2010). A catalog of felt intensity data for 589 earthquakes in India, 1636–2009, *Bull. Seismol. Soc. Am.* **100,** no. 2, 536–569, doi: 10.1785/0120080328.

Medvedev, S. V., W. Sponheuer, and V. Kárník (1965). *Seismic Intensity Scale Version MSK 1964*, Akademii Nauk SSSR Geofiz. Kom., Moscow, 280 pp. (in Russian).

Middlemiss, C. S. (1910). *The Kangra Earthquake of 4th April 1905*, Memoirs of the Geological Survey of India, Vol. 38, 409 pp. (1981 reprint), Calcutta, India.

Min, Z. (Editor) (1995). *Catalogue of Historic Strong Earthquakes in China: 23rd Century to 1911 A.D.*, Seismological Press, Beijing, China, 529 pp. (in Chinese).

Molnar, P, and D. Qidong (1984). Faulting associated with large earthquakes and the average rate of deformation in central and eastern Asia, *J. Geophys. Res.* **89,** 6203–6227, doi: 10.1029/JB089iB07p06203.

Musson, R. (1998). Intensity assignments from historical earthquake data: Issues of certainty and quality, *Ann. Geofsc.* **41,** no. 1, 79–91.

Musson, R. M. W., G. Grunthal, and M. Stucchi (2010). The comparison of macroseismic intensity scales, *J. Seismol.* **14,** 413–428, doi: 10.1007/s10950-009-9172-0.

Nepal Residency Records (IOR/R/5/95-96), *India Office Records*, British Library, London, United Kingdom.

Nobuo, T., K. Sawada, M. Shigefugi, S. M. Bijukchhen, M. Ichiyanagi, T. Sasatani, Y. P. Dhakal, S. Rajaure, and M. R. Dhital (2015). Shallow underground structure of strong ground motion observation sites in the Kathmandu valley, *J. Nepal Geol. Soc.* **48,** 66.

Pant, M. R. (2002). A step towards a historical seismicity of Nepal, *Adarsa (Supplement to the Purnima Journal)*, Series II, Vol. 2, Samshodhana Mandal, Pundit Publications, Kathmandu, Nepal, 29–60.

Parkes, F. (1950). *Wanderings of a Pilgrim in Search of the Picturesque, during Four and Twenty Years in the East; with Revelations of Life in the Zenana*, Pelham Richardson, London, United Kingdom, 285 pp.

Rana, B. S. J. B. (1934). *The Great Earthquake in Nepal*, K. Lal (Editor), 2013, Ratna Pustak Bhandar, Kathmandu, Nepal, 237 (in Nepali).

Sapkota, S. N., L. Bollinger, Y. Klinger, P. Tapponier, Y. Gaudemer, and D. Tiwari (2013). Primary surface rupture of the great Himalayan earthquakes of 1255 and 1934, *Nature Geosci.* **6,** 71–76, doi: 10.1038/ngeo1669.

Szeliga, W., S. E. Hough, S. Martin, and R. Bilham (2010). Intensity, magnitude, location, and attenuation in India for felt earthquakes since 1762, *Bull. Seismol. Soc. Am.* **100,** 570–584, doi: 10.1785/0120080329.

Wald, D. J., V. Quitoriano, L. Dengler, and J. W. Dewey (1999). Utilization of the Internet for rapid community intensity maps, *Seismol. Res. Lett.* **70,** no. 6, 680–697, doi: 10.1785/gssrl.70.6.680.

Wessel, P., and W. H. F. Smith (1999). Free software helps map and display data, *Eos Trans. AGU* **72,** 441, 445, doi: 10.1029/90EO00319.

***Stacey S. Martin***
***Earth Observatory of Singapore (EOS)***
***Nanyang Technological University***
***50 Nanyang Avenue, N2-01a-14***
***Singapore 639798***
***7point1@gmail.com***

***Susan E. Hough***
***United States Geological Survey (USGS), Pasadena***
***525 South Wilson Avenue***
***Pasadena, California 91106 U.S.A.***
***hough@usgs.gov***

***Charleen Hung***
***Ring am Feld 48***
***14532 Kleinmachnow, Germany***